Long-Ranged Oppositely Charged Interactions for Designing New Types of Colloidal Clusters

Ahmet Faik Demirörs*,†,‡, Johan C. P. Stiefelhagen†, Teun Vissers,†,‡ Frank Smallenburg‡, Marjolein Dijkstra, Arnout Imhof and Alfons van Blaaderen*

[1] *Soft Condensed Matter, Debye Institute for Nanomaterials Science, Department of Physics, Utrecht University, Princetonplein 5, 3584 CC Utrecht, The Netherlands*

*Correspondence should be addressed to; A.F. Demirörs, A.F.Demirors@gmail.com, A. van Blaaderen A.vanBlaaderen@uu.nl

† Authors contributed equally.

‡ Present addresses: Department of Materials, ETH Zurich, 8093 Zurich, Switzerland (A.F.D.)

Institut für Theoretische Physik II - Soft Matter Heinrich-Heine-Universität Düsseldorf, Germany (F.S.)

University of Edinburgh, James Clerk Maxwell Building, Mayfield Road, Edinburgh (T.V.)

Fabrication of Titania colloids and Stöber silica particles

Titania colloids were synthesized according to the procedure of Yu et al.[1] Particles synthesized were calcined at 500 °C for 2h, which resulted in a phase transition to anatase titania. Silica particles used here were synthesized with a modified Stöber seeded growth method as described by Zukoski and co-workers.[2] these particles were labelled with fluorescent dye according to the procedure of van Blaaderen.[3]

Synthesis of PMMA particles

The PMMA particles in this thesis were synthesized using a dispersion polymerization method described by Bosma *et al.*[4] During the synthesis, the particles were sterically stabilized with poly-12-hydroxystearic acid (PHSA) grafted on a PMMA backbone.[4] A fluorescent dye, rhodamine isothiocyanate (RITC) or 7-nitrobenzo-2-oxa-1,3-diazol (NBD) or Coumarine, was covalently incorporated in the polymer backbone. Occasionally, the PMMA backbone of the comb-graft stabilizer was covalently bound to the surface in an additional locking step. Finally, the particles were washed several times with hexane to remove unreacted substances that were present as left-overs in the reaction-mixture (e.g. dodecane, traces of acetone, unreacted monomer). In each washing step, the particles were first centrifuged after which the supernatant was removed, and the particles were redispersed in hexane. This process was repeated for typically three times.

Locking PMMA particles

Repeated washing steps may remove the stabilizer, rendering the particles unstable. When particles were desired that remain stable in solution even after many centrifugation/washing steps, the stabilizer was covalently bonded to the methacrylic acid molecules at the surface of particles. This procedure is called the locking step. The epoxy-rings in the glycidyl methacrylate units in the backbone of the stabilizer are opened using 2-di-methylaminoethanol. They can then connect to the -OH groups of the methacrylate (MA) units at the surface of the particles. If this locking step was performed immediately after synthesis of the particles, an amount of dodecane equal to the weight of hexane already in the suspension was added to the flask. If older and possibly dried particles were to be locked, an amount of dodecane approximately similar to the combined weight of hexane and dodecane used in the initial synthesis was added. This amounts to approximately 50 weight percent particles in dodecane. If the particles had been washed many times in hexane already and stabilizer molecules might have desorbed, the dodecane was saturated with stabilizer solution before use. To this end a stock solution was prepared by adding approximately 1 g of stabilizer solution to 20 mL of dodecane and thoroughly vortexing. Excess stabilizer was allowed to sediment and the dodecane to be used was taken from the top of the vial. It is estimated that this dodecane contained on the order of 0.1 wt% stabilizer polymer. By slowly raising the temperature of the flask to 130 °C without connecting a reflux condenser any residual hexane was evaporated. Next, the ring opener 2-dimethylaminoethanol was added (≈2.5 μL/g PMMA particles), the reflux condenser was attached again and the reaction allowed to proceed for 2 hours. The synthesis was then washed with hexane as described above. In the case of RAS labelled particles, upon ring opener addition, the particles were observed to become paler during the reaction. This is likely due to the basicity of 2-dimethylaminoethanol. This bleaching effect also resulted in less fluorescence, as in the confocal microscope such particles emitted less light. With NBD labelled particles this effect was not observed.

Negatively charged PMMA particles with phosphoric acid 2-hydroxyethyl methacrylate (PAM)

PMMA particles produced with the procedure of Bosma *et al.*[4] normally acquire a positive charge when dispersed in cyclohexylbromide (CHB) or a mixture of CHB and cis-decalin (cis-dec). However, the positive charge can be altered by adding acidic groups to the synthesis, some of which end up at the particle surface. Charge conversion from positive to negative becomes possible when these acidic groups can dissociate in the solvent chosen. When a sufficient amount of these groups dissociate, the surface of the particles can become negatively-charged. Similar acid/base interactions were described by Poovarodom *et al.*,[5,6] who showed that adding a basic surfactant to an apolar solvent increased the electrophoretic mobility of negatively charged acid-functionalized sterically stabilized particles. In our case, embedding phosphoric acid 2-hydroxyethyl methacrylate (PAM) into the PMMA synthesis caused the particles in CHB/cis-Dec to

become negatively charged when they were dispersed together with other particles to which they could donate protons.

The synthesis of PAM-PMMA particles was performed in a core shell fashion by using positively-charged PMMA particles as seeds. In a 5 mL round bottom flask a magnetic stir bar was placed. In this flask 0.500 g of NBD labelled core particles ($\sigma = 1040$ nm) were weighed. In a 20 mL vial a mixture containing 65.5 wt% hexane, 30.6 wt% dodecane, and 3.9 wt% acetone was prepared and homogenized. 1.003 g of this mixture was added to the core particles. The core mixture was placed on a magnetic stirrer and stirred for half an hour to properly disperse all core particles. Next, 0.0487 g stabilizer solution and 0.032 g azobisisobutyronitrile (AIBN) were added, after which the reactants were allowed to stir while in the mean time the feed was prepared. The feed was prepared in a 4 mL vial by adding 1.003 g methylmethacrylate (MM), 0.030 g methacrylic acid (MA), 0.010 g PAM, approximately 1 mg 4-methylaminoethyl methacrylate-7-nitrobenzo-2-oxa-1,3-diazol (NBD-MAEM), 0.2503 g hexane/dodecane/acetone mixture and 8 μL 1-octanethiol. The vial was then vortexed to homogenize its contents. With this feed mixture a 1 mL syringe was filled and placed in the syringe pump, which was programmed to add 850 μL of the feed to the core mixture in units of 50 μL each spaced apart 2 minutes and 56 seconds in time. This way the total addition time amounted to 50 minutes. After the addition the reaction was allowed to continue for 2 more hours. The reaction temperature was 83 °C and the stirring rate was set at 200 rpm. The carousel was allowed to cool down, particles were washed three times in hexane and dried. The total diameter of the particles after this step was $\sigma = 1380$ nm, indicating that the shell containing PAM had a thickness of ca. 165 nm.

Positively charged silica particles

Positively charged silica particles were made by using the same comb grafted stabilizer consisting of poly(12-hydroxystearic acid) (PHSA) mentioned above. 3 drops of PHSA stabilizer (0.347 g/mL solution in ethyl acetate and butyl acetate with a 2:1 mass ratio, respectively) was added to a silica dispersion, which was coated with an extra silica layer in tetrahydrofuran (THF). Thus PHSA groups were physisorbed or partially embedded into the extra silica layer coating the surface. This additional grown silica layer was only tens of nanometers thick and was made by adding 50-100 μL of TEOS in to a 10 mL 1.1μm silica particle dispersion in THF with a concentration of 5%(v/v). To this dispersion a 50 μL of NH_3 (ammonia used throughout this paper was 28-30% concentrated aqueous solution) aliquot was added before the TEOS addition to catalyze the reaction.

Clusters of silica particles

Positively-charged silica particles prepared as described above were centrifuged a few times and resuspended in THF. Negatively-charged silica particles were dried from ethanol dispersions and resuspended in THF by sonication and

vortex. A concentrated dispersion of negatively-charged silica particles (N) was added an aliquot of positively-charged silica particles (P) to provide a particle number ratio of N_N:N_P = 10:1, where N_N is the number of negatively-charged silica particles and N_P is the number of positively-charged silica particles. Total particle concentration of the mixture of oppositely-charged particles was 5% (v/v). The addition of NH_3 solution to the solution decreases the screening length but 50 μL of NH_3 for a total 10 mL of THF keeps the soft inter-cluster-repulsions enough such that the clusters stay stable. This amount of NH_3 was sufficient to catalyze the extra silica growth over the clusters to permanently fix them.

Clusters of PMMA particles

To create clusters of oppositely charged PMMA particles, positively and negatively charged PMMA particles were required. By incorporating the acidic monomer phosphoric acid 2-hydroxyethyl methacrylate (PAM) into particles, we could create particles that were negatively charged in CHB/decalin even at low volume fractions when they were surrounded by many normal PMMA particles. The negative charge of these particles stems from the acidic PAM molecules incorporated in the particles. When these PAM molecules can donate sufficient H^+ ions to the solvent and/or to other PMMA particles with a different composition, this renders the particles negatively charged. The positive charge of the normal PMMA particles likely stems from H^+ ions that adsorb onto the particles in an excess compared to negative ions, such as Br^-. It is quite likely that these originate from a slight decomposition of CHB. However, in our case, they can also be donated by the PAM molecules of the particles of the opposite type. The negatively charged PMMA particles were always fluorescently labelled with an NBD dye (green in the images) whereas the larger positively charged PMMA particles contained RAS as a fluorescent label (red in the images).

Effect of salt and shear on clusters of oppositely charged PMMA colloids

We studied the effect of salt concentration and stirring on mixtures of locked positively charged particles (type B, red, σ_B = 4025 nm) and locked negatively charged PAM-PMMA particles (type A, green, σ_A = 1380 nm). The size ratio σ_B:σ_A is 3:1, which geometrically ensures that no more than four of the larger satellite particles (B) can be touching one smaller center particle (A). To this end, a solvent mixture was prepared consisting of 27.2 wt% cis-decalin (cis-dec) and 72.8 wt% cyclohexylbromide (CHB). The conductivity of this mixture was measured to be 64 pS/cm. Using this solvent mixture in two 2 mL vials suspensions were made: one containing 10 vol% locked particles B (σ = 4025 nm) and one containing 1 vol% 1380 nm locked PMMA particles A (σ = 1380 nm). Both suspensions were thoroughly vortexed and left to equilibrate overnight, after which they were thoroughly vortexed again. A few days later, in a third 2 mL vial a mixture of the two suspensions was prepared by adding 0.2752 g suspension with particles B to 0.0104 g of suspension with particles A. Given the individual volume fractions and the particles diameters this gives a

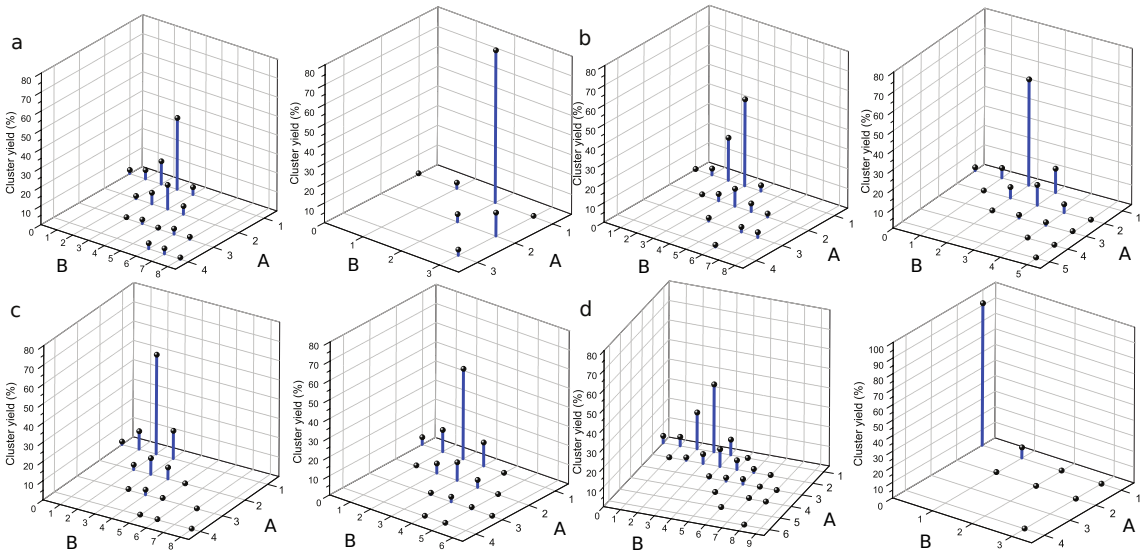

Figure S1. The effect of salt concentration and stirring on cluster yields for mixtures containing positively charged PMMA particles (type B, red, $\sigma = 4025$ nm) and locked negatively charged PAM-PMMA particles (type A, green, $\sigma = 1380$ nm). The vertical axis gives the cluster yield. The axis that goes up to 9 denotes the number of satellite particles (type B, red) whereas the other axis gives the number of central particles (type A, green). (**a**) Normalized incidence of clusters found in a suspension without added salt (left) before and (right) after stirring, (**b**) Normalized incidence of clusters found in a suspension with a TBAB salt concentration of approximately 0.5 μM, (left) shows the sample before and (right) after stirring, (**c**) Normalized incidence of clusters found in a suspension with a TBAB salt concentration of approximately 1 μM, (left) shows the sample before and (right) after stirring, (**d**) Normalized incidence of clusters found in a suspension with a TBAB salt concentration of approximately (left) 1.5 μM and (right) 2.0 μM. Both of these samples were analyzed after stirring.

number ratio N_B:N_A = 10:1 at a volume fraction of (just below) 10%. This suspension was homogenized by vortexing, after which a small magnetic stir bar was added.

In a separate 2 mL vial, a solution was prepared of 0.1005 g CHB, saturated with tetrabutylammonium bromide (TBAB). The saturation value of TBAB-in-CHB is known to be approximately 260 μM.[7] This TBAB-saturated CHB was diluted with 0.9075 g CHB/cis-dec mixture. Over the course of several days, appropriate amounts of diluted TBAB-in-CHB were added to the vial containing the particle mixture to create suspensions with salt concentrations ranging from 0 to 2 μM. The Debye screening lengths κ^{-1} for TBAB concentrations of 0, 0.5, 1, 1.5, and 2 μM are estimated to be 2.0, 1.3, 1.0, 0.9, and 0.8 μm. Some samples were prepared immediately after homogenizing the suspension by thorough vortexing, others after prolonged stirring of the suspension.

Figure S1 shows the cluster yield of various types of clusters at different concentrations of the salt TBAB before or after stirring. The type of cluster is defined by the number of central (green, type A) particles and the number of satellite particles (red, type B) that are attached to them. The cluster yield for a certain cluster type is then given by the fraction of the maximum number of these clusters that could have formed given the total number of green particles in the suspension. Figure S1a shows the cluster distribution in a sample that contained no tetrabutylammonium bromide (TBAB), just after the suspension had been homogenized. Without stirring, a large distribution of cluster

sizes was found with the highest peak located at the AB_3 configuration. After stirring the suspension at 400 rpm overnight, the cluster distribution was analyzed again (Figure S1a right hand side) and displayed a clear preference for AB_2 clusters (almost 80% yield). The configuration shift from AB_3 to AB_2 can also be observed for a salt concentration of 0.5 μM, see Figure S1b. For salt concentrations of 1.0 μM (Figure S1c) and 1.5 μM (Figure S1d, graph on the left), after stirring AB_3 clusters were more abundant than for the lower salt concentrations. When the TBAB concentration was increased further to 2.0 μM the particles were no longer oppositely charged (Figure S1d, graph on the right). The differences in cluster distributions before and after stirring are most likely an effect of the shear, which breaks and redistributes some of the satellite particles. The process of cluster formation is an example of an out-of-equilibrium process and the path taken will depend of parameters such as shear. However, we did find that the process was reproducible if repeated under the same conditions.

Finally, a similar effect of shear on the cluster type was also observed for the silica particles. In this case, a half-filled 20 mL vial that was placed on a roller bank at a higher speed (180 rpm) than during the fixing by silica-coating (120 rpm). The prefered cluster type shifted from tetrahedra to triangles. The two types of shear experiments for PMMA and silica particles are not directly comparable but seem to show a qualitative trend for the influence of shear on the cluster size.

Preparation of clusters of oppositely charged colloids with size ratio satellite:core=2.2:1 (sample 7)

We also prepared clusters using a particle mixture of PMMA particles type A and B with size ratio σ_B:σ_A = 2.2:1 (sample 7 in main text). For this, a 0.4168 g/g suspension of positively-charged PMMA particles (σ_B = 3025 nm, red) in cis-decalin and a 0.0317 g/g suspension of negatively-charged PAM-PMMA particles (σ_A = 1380 nm, green) in cis-decalin were prepared in two separate 2mL glass vials. In a third 2 mL glass vial 0.2262 g of particles B suspension was added to 0.0273 g of particle suspension A, after which the vial was thoroughly vortexed. Next, the vial was held onto the vortexer without cap, while dropwise 0.4300 g CHB (conductivity σ = 455 pS/cm) was added. As a consequence, the number ratio in the sample N_B:N_A was approximately 10:1, while the total volume fraction was approximately 14%. The sample was prepared and studied with confocal microscopy 24 hours after preparation.

Confocal sample preparation and observation

Samples were prepared by filling 0.1 x 2.0 x 33.3 mm glass capillaries with suspension and placing them on a glass microscope slide. Capillaries were sealed by placing a drop of UV curable glue (Norland optical adhesive #68) on both ends of a capillary. A UV lamp (peak wavelength $\sim$ 365nm) was used to cure the glue for approximately 10 minutes,

while the middle part of capillaries was shielded against UV exposure by a piece of aluminium foil.

Samples were observed using a Nikon C1 or Leica SP2 confocal microscope mounted on a Leica DMIRB frame with a 63x oil immersion objective. Clusters that were deemed interesting were zoomed in on and a Z-stack consisting of 59 images was recorded at an XY-resolution of 160 x 80 pixels to accurately observe their structure. A stack would generally span a box of approximately 25 x 12 x 12 μm. The relatively low resolution ensured a faster scanning speed and since the scanhead was zoomed in on only one cluster, this still yielded enough pixels per particle to extract particles' coordinates with reasonable accuracy.

For the samples with varying salt concentration larger Z-stacks were recorded to investigate the distribution of various types of clusters. One or more Z-stacks were recorded at a XY-resolution of 256 x 256 pixels at a zoom level that spanned approximately 100 x 100 μm. These settings allowed for reasonably fast confocal scanning, to minimize tracking errors. The size of the scanned box ensures the recording of typically more than 5000 particles, while the resolution is still high enough for tracking software to identify the particles' positions.

Confocal data analysis

Coordinates of the particles were obtained from 2D and 3D confocal microscopy images using an algorithm similar to the method described by Crocker and Grier,[8] but extended to 3D as e.g. described in Refs. 9, 10. Output files consisting of a list of the identified particles' X, Y and Z coordinates were visualized using OpenGL software.

Cluster analysis

To analyze the amounts of clusters that had formed and their composition, a program was written in C, which analyzed coordinate files. Touching particles were identified as particles for which distance d_{ij} matched the following criterium:

$$|r_{\mathrm{i}} - r_{\mathrm{j}}| < d_{\mathrm{ij}} < 1.15 \cdot (r_{\mathrm{i}} + r_{\mathrm{j}}) \tag{1}$$

Here, d_{ij} is the distance from a particle i to a particle j, r_{i} is the radius of particle i and r_{j} is the radius of particle j. The factor of 1.15 was found to be a suitable upper threshold below which particles were still deemed to be touching. The lower threshold ensures that in the visualisation, a particle should at least stick out visibly from another particle's surface. Both thresholds compensate for tracking errors that arise from particles having moved due to Brownian motion in the time interval between the acquisition of consecutive XY-slices.

Two particles that are considered to be touching, but that are of the same type (i.e., both A or both B), without another particle of the other type attached to it, are not counted as clusters as they did not form due to attraction between opposite charges. From the confocal images we estimate that approximately 4% of green particles had formed such dumbbell particles. The configuration of two same-type particles touching is most likely due to aggregation before

dispersing the particles, but sometimes can also be a false positive in the determination of the particle positions from the confocal images.

AB_7 and AB_9 Clusters

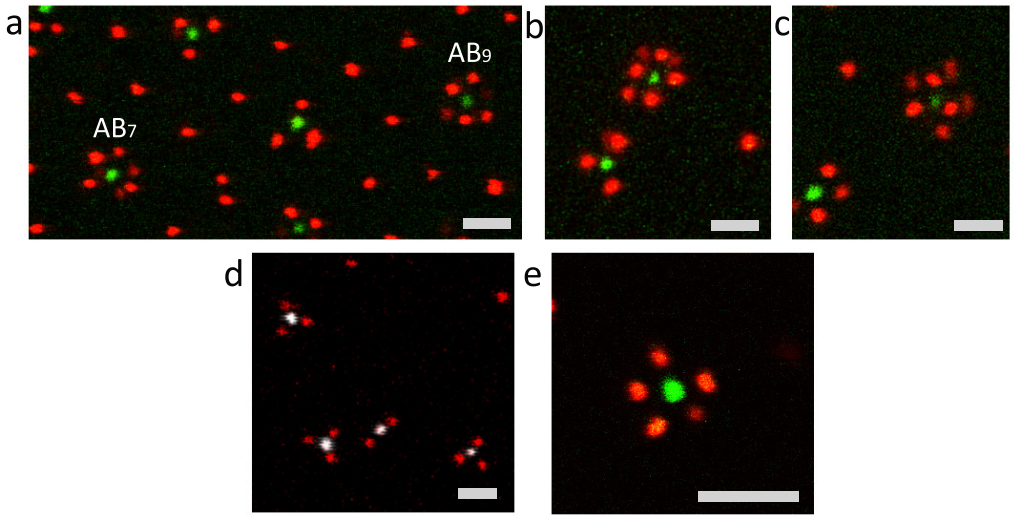

Figure S2. Confocal microscopy images of silica-silica oppositely charged clusters with AB_7 and AB_9 structures, found in a mixture of 1.1 μM positively charged silica and 1.3 μM negatively charged silica particles: a) an image shows both these clusters together, and b) and c) are the images of AB_9 clusters at different times. See also the Supplementary movie S5. d) This is a confocal image of NH_3 like particles clusters formed by the detachment of one satellite particle, see also Supplementary movie S6. e) Another broken cluster that became AB_5 after losing some satellites, see also Supplementary movie S7. Scale bars are 2 μm.

While experimenting with 1.1 μM positively charged silica and 1.3 μM negatively charged silica particles we have also observed higher order clusters like AB_7 and AB_9 clusters, (see Figure S2a, b, c). These clusters were observed when we had a higher number ratio of N_B:N_A = 20. It was hard to determine the structure of these clusters with confocal data analysis but the confocal movie helps to visualize the 3D structure, see Supplementary movie S5 for these clusters. Here we also demonstrate two examples of clusters with broken satellite particles; Fig S2d is the confocal image of NH_3 like particle clusters, see also Supplementary movie S6. Fig S2e is another broken cluster that is AB_5 after breaking of some satellites, see also Supplementary movie S7.

Influence of satellite:central particle number ratio on the clusters

When the number ratio between satellite particles B and core particles A was decreased from N_B:N_A=10:1 to N_B:N_A=2:1, the clusters grew in size and formed ring or chain-like structures. An example for negatively charged silica particles (σ_B = 1.1 μm, red) and positively charged titania particles (σ_A = 1 μm, green) in THF is given in Figure S3. The distance in between these structures shows that there is still a net electrostatic repulsion between

them. We never observed chain-like particles transform into clusters. However, the formation of smaller clusters could have occurred in the brief period before the samples were studied under the microscope. In any case, the appearance of chains and rings at lower number ratios already suggests that the clusters formed at higher number ratios (N_B:N_A=10:1) were not the equilibrium structures. However, provided that satellite particles are in sufficient excess to saturate all core particles, metastable clusters such as in Fig. 2 of the main text could be reproducibly created.

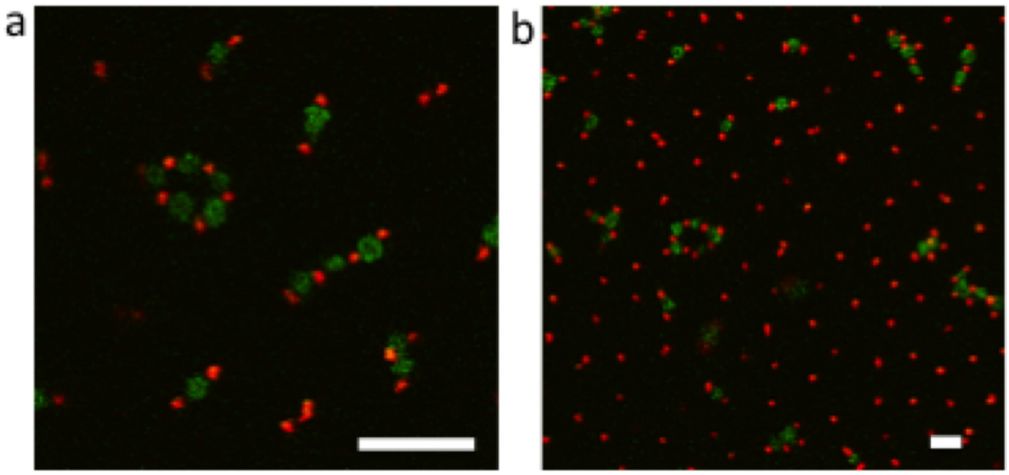

Figure S3. Negatively charged silica particles ($\sigma_B = 1.1$ μm, red) and positively charged titania particles ($\sigma_A = 1$ μm, green) in THF with a core:satellite number ratio of approximately 1:2 form ring and chain-like structures. Confocal microscopy image of positively-charged titania particles and negatively-charged silica particles dispersed in THF are given in a zoomed-in example to show the alternating sequence of positive-negative particles in the chain and ring structures (a) and in a zoomed-out example to demonstrate the long-ranged repulsions between the clusters and free satellite particles. Scale bars are 4 μm.

Some examples of found cluster configurations

In the figure below, we show an overview of observed cluster configurations in the experiments of green (g, type A) and red (r, type B) particles. For higher numbers, e.g., B=4, A=3, more than one isomer may exist.

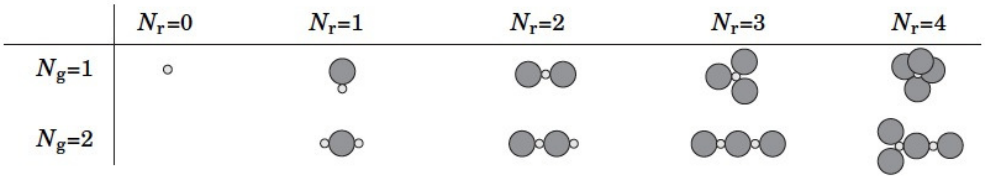

Figure S4. Some schematic examples of lower number clusters for one and two central particles.

Clusters of large core particles and small satellite particles

Particle synthesis

Large negatively charged PMMA colloids ($\sigma_{\mathrm{L}} = 3.68$ μm) and small positively charged PMMA colloids ($\sigma_{\mathrm{S}} = 0.64$ μm) formed clusters of oppositely charged particles (see Fig. 4 of the main text). Both the large and small particles were synthesized by dispersion polymerization.[4] The large particles were labeled with NBD (color-coded green in the images) whereas the small particles were labeled with RITC (red in the images). During the synthesis of the small particles, an additional 2.5w% of 2-(dimethylamino)ethylmethacrylate was added to the reaction mixture. As a result, the small particles readily acquire and retain a positive charge upon mixing them with the large particles in CHB/cis-decalin.

Estimating the charge of the particles and the charge of the clusters

From the confocal microscopy images, we used particle tracking to measure the electrophoretic mobilities of the loose small particles and clusters of large and small particles while they were moving in an electric field. The electrophoresis experiments were performed inside a glass capillary (Vitrocom, 0.1 x 2.0 mm cross-section) with two conductive wires threaded along either side (see Ref. 11 for more details about the experimental setup). We note here that because of sedimentation effects, the large clusters were mainly found close to the lower capillary wall. For this reason, the movies with the clusters of large and small particles (Fig. 4 in main text, supplementary movies 8-11) were recorded ~ 8 μm above the lower capillary wall. This is below the lower stationary layer [i] (located ca. 20 μm above the lower wall for the capillary used) where the macroscopic flows in the capillary channel that arise because of the electric field cancel each other.[11,12] Filling in electrophoretic mobilities of the small particles $\mu_{\mathrm{S}} = 200$-300 μm^2/Vs, we calculated the particle charge either ignoring effects of overlapping electrical double layers, or by using a method for concentrated dispersions of particles in low-polar solvents that takes these effects into account.[12] The results are summarized in Table S1 and show how the calculated particle charge varies with the volume fraction that is used as input. The charge on the small particles roughly falls in a range between $Z_{\mathrm{S}}e = +25e$ (lower bound estimate when assuming a dilute dispersion) and $Z_{\mathrm{S}}e = +100e$ (higher bound estimate by taking into account effects of volume fraction and thick double layers). More information can be found in Refs. 11–13.

The electrophoretic mobility of the clusters was taken to be in the range $\mu_{\mathrm{tot}} = 200 - 400$ μm^2/Vs (the higher bound of this range was taken considering the fact that the movies were recorded below the stationary layer). When we regard the clusters as large spherical particles with radius $a_{\mathrm{tot}} = \sigma_{\mathrm{L}}/2 + \sigma_{\mathrm{S}} = 2.48$ μm and use the expression $Ze = 6\pi\eta\mu_{\mathrm{tot}}a(1+\kappa a)/f(\kappa a)$, with $f(\kappa a)$ the Henry correction factor,[11] and values for the viscosity $\eta \approx 2.7$ mPa·s

[i] When an electric field is applied inside the capillary, ions near the capillary wall are put into motion and drag the fluid with them to cause a plug flow, a process called electro-osmosis. Because the fluid is incompressible and the capillary is sealed, a Poiseulle flow counteracting the electro-osmotic flow arises. These two flows cancel each other at two planes in the capillary called the stationary layers.[12]

Table S1 Estimates of the charge on the small particles with and without taking into account the effect of overlapping double layers. Calculations were performed for a given value of the electrophoretic mobility, a screening length $\kappa^{-1} = 1.82$ μm, viscosity $\eta \approx 2.7$ mPa·s and relative permittivities for medium $\epsilon_{\mathrm{medium}} = 5.6$ and particle $\epsilon_{\mathrm{particle}} = 2$. Although the average volume fraction in the sample was $\phi = 0.02$, we also took into account a higher volume fraction (the actual volume fraction in the lower part of the capillary might have been slightly higher due to sedimentation effects) to get an upper bound on the estimated particle charge.

Method	Volume fraction ϕ	Electrophoretic mobility μ_{S} [μm^2/Vs]	Particle charge Z_{S} [e]
$Ze = 6\pi\eta\mu_{\mathrm{S}}a(1+\kappa a)/f(\kappa a)$	-	200	+24
$Ze = 6\pi\eta\mu_{\mathrm{S}}a(1+\kappa a)/f(\kappa a)$	-	300	+36
Method in Ref. 12	10^{-6}	200	+18
Method in Ref. 12	10^{-6}	300	+28
Method in Ref. 12	0.02	200	+58
Method in Ref. 12	0.02	300	+76
Method in Ref. 12	0.04	200	+81
Method in Ref. 12	0.04	300	+100

and Debye screening length $\kappa^{-1} \approx 1.82$ μm, we can estimate $Z_{\mathrm{tot}}e$ in a range between $+200e$ and $+1000e$.

By assuming that the charges are additive, we can gauge the charge on the large particles as the average of the estimated cluster charges minus the average of the estimated charges on the satellite particles. Given that the clusters typically contained approximately 60 small particles, taking the average values for the charges yields: $Z_{\mathrm{L}}e = Z_{\mathrm{tot}}e - Z_{\mathrm{S}}e$=(200$e$+1000$e$)/2-(25$e$*60+100$e$*60)/2 = -3150$e$. In the case of taking the highest estimate for the charge on the small particles and lowest for the cluster as a whole, one obtains: 200e-100e*60=-5800e, the lowest estimate for the small particles and highest for the cluster as a whole one obtains 1000e-25e*60 = -500e. Taking into account this considerable spread, $Z_{\mathrm{L}}e = -3150e \pm 2650e$ seems a reasonable estimate for the charge on the large particle.

Debye screening length

The Debye screening length was estimated from the measured conductivity of the solvent (27.2 w% cis-decalin / 72.8 w% CHB, $\sigma = 70$ pS/cm). The conductivity measurements were used to calculate the ionic strength. From the ionic strength, we estimated the Debye screening length $\kappa^{-1} = 1.82$ μm. More details can be found in Refs. 13–15.

Charge inversion of the clusters in an electric field at $|E| = 77$ V/mm

We extracted the electrophoretic mobility for the clusters moving in an electric field of $|E| = 77$ V/mm from the confocal microscopy data corresponding to movie S11 (ca. 8 μm above the lower capillary wall). Images from this movie are shown in Fig. S5 (same as in Fig. 4iii in the main text). The corresponding electrophoretic mobility for the clusters inside the field of view is shown in Fig. S5j. As small particles got pulled off, the cluster as a whole became negatively charged and the electrophoretic mobility flipped sign.

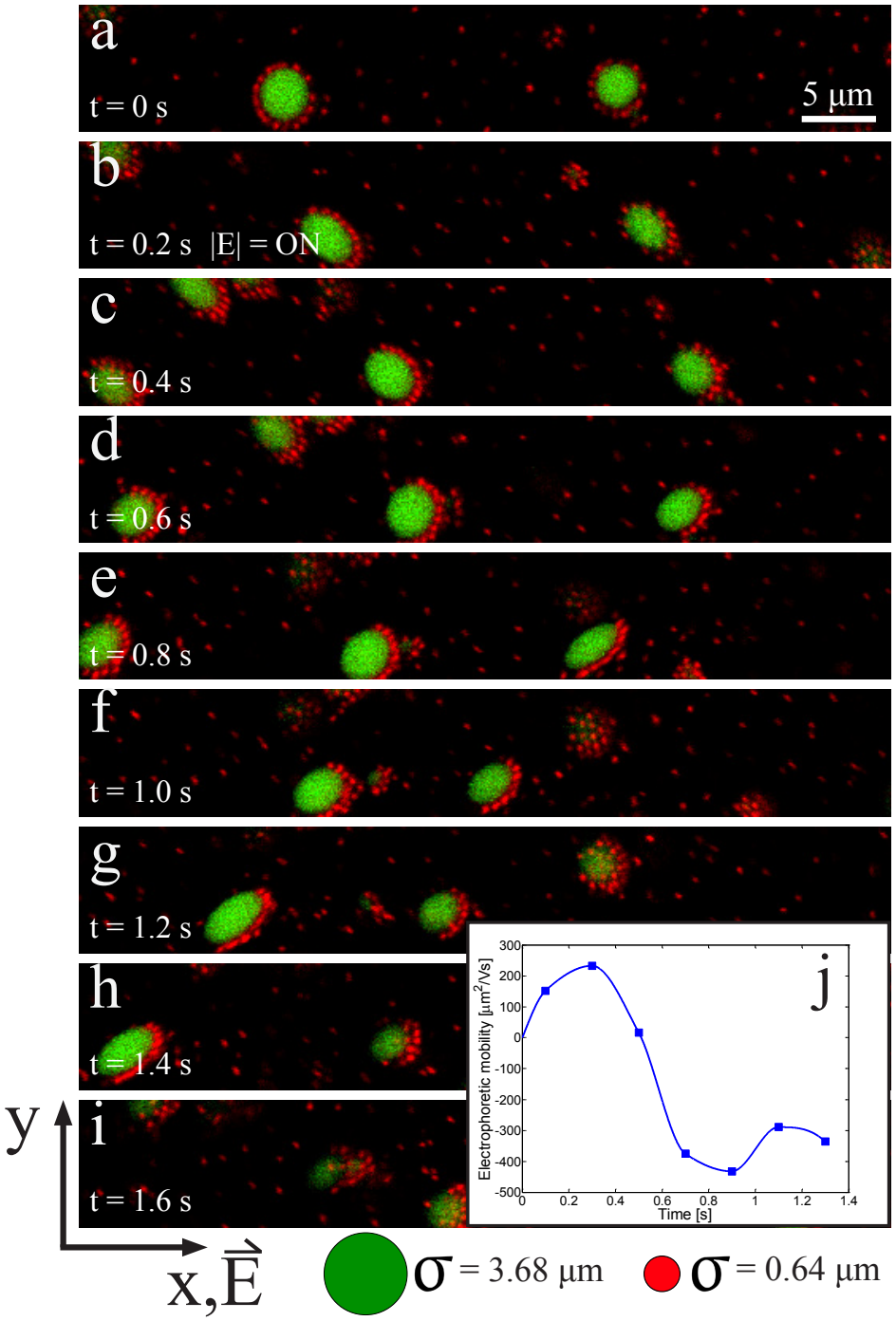

Figure S5. Confocal microscopy images from a time series at $|E| = 77$ V/mm. (a-i:) (same as main text Fig.4iii) In the first image (a), no field was applied. During the first ~ 0.6 s in which the field was applied, clusters moved towards the negative electrode (b-d). Small particles (red) accumulating on one side of the large particle (green) caused an anisotropic charge distribution on the cluster. At some point between 0.4 s and 0.6 s after the field was turned on (d,e), the clusters as a whole reversed direction (e-i), indicating that a sufficient number of small particles had been pulled from the large particle by the electric field to reverse the net charge of the cluster. (j:) the electrophoretic mobility of the clusters becomes negative when the charge on the clusters reverses and they start to move towards the positive electrode. The blue line is a guide to the eye.

References

[1] Yu, H. K.; Yi, G. R.; Kang, J. H.; Cho, Y. S.; Manoharan, V. N.; Pine, D. J.; Yang, S. M. *Chemistry of Materials* **2008**, *20*, 2704–2710.

[2] Bogush, G.; Tracy, M.; Zukoski, C. *Journal of Non-Crystalline Solids* **1988**, *104*, 95–106.

[3] van Blaaderen, A.; Vrij, A. *Langmuir* **1992**, *8*, 2921–2931.

[4] Bosma, G.; Pathmamanoharan, C.; de Hoog, E.; Kegel, W. K.; van Blaaderen, A.; Lekkerkerker, H. *Journal of Colloid and Interface Science* **2002**, *245*, 292–300.

[5] Poovarodom, S.; Poovarodom, S.; Berg, J. C. *Journal of Colloid and Interface Science* **2010**, *351*, 415–420.

[6] Poovarodom, S.; Berg, J. C. *Journal of Colloid and Interface Science* **2010**, *346*, 370–377.

[7] Sanz, E.; Leunissen, M. E.; Fortini, A.; van Blaaderen, A.; Dijkstra, M. *The Journal of Physical Chemistry B* **2008**, *112*, 10861–10872.

[8] Crocker, J. C.; Grier, D. G. *Journal of Colloid and Interface Science* **1996**, *179*, 298–310.

[9] Dassanayake, U.; Fraden, S.; van Blaaderen, A. *The Journal of Chemical Physics* **2000**, *112*, 3851–3858.

[10] Jenkins, M.; Egelhaaf, S. *Advances in Colloid and Interface Science* **2008**, *136*, 65–92.

[11] Vissers, T.; Wysocki, A.; Rex, M.; Lowen, H.; Royall, C. P.; Imhof, A.; van Blaaderen, A. *Soft Matter* **2011**, *7*, 2352–2356.

[12] Vissers, T.; Imhof, A.; Carrique, F.; Delgado, Á. V.; van Blaaderen, A. *J Colloid Interface Sci* **2011**, *361*, 443–55.

[13] Vissers, T. Oppositely charged colloids out of equilibrium. 2010; http://dspace.library.uu.nl/handle/1874/188014.

[14] van der Linden, M. N.; Stiefelhagen, J. C. P.; Heessels-Grboa, G.; van der Hoeven, J. E. S.; Elbers, N. A.; Dijkstra, M.; van Blaaderen, A. *Langmuir* **2015**, *31*, 65–75.

[15] Yethiraj, A.; van Blaaderen, A. *Nature* **2003**, *421*, 513–517.